Biochemical and Biophysical Research Communications 439 (2013) 564–569

Contents lists available at ScienceDirect

Biochemical and Biophysical Research Communications

journal homepage: www.elsevier.com/locate/ybbrc

Molecular basis for homo-dimerization of the CIDE domain revealed by the crystal structure of the CIDE-N domain of FSP27

Seung Mi Lee, Tae-ho Jang, Hyun Ho Park *

School of Biotechnology and Graduate School of Biochemistry at Yeungnam University, Gyeongsan, South Korea

ARTICLE INFO

Article history:
Received 23 August 2013
Available online 8 September 2013

Keywords:
Apoptosis
Energy metabolism
FSP27
Crystal structure
CIDE domain

ABSTRACT

FSP27 (CIDE-3 in humans) plays critical roles in lipid metabolism and apoptosis and is known to be involved in regulation of lipid droplet (LD) size and lipid storage and apoptotic DNA fragmentation. Given that CIDE-containing proteins including FSP27 are associated with many human diseases including cancer, aging, diabetes, and obesity, studies of FSP27 and other CIDE-containing proteins are of great biological importance. As a first step toward elucidating the molecular mechanisms of FSP27-mediated lipid droplet growth and apoptosis, we report the crystal structure of the CIDE-N domain of FSP27 at a resolution of 2.0 Å. The structure revealed a possible biologically important homo-dimeric interface similar to that formed by the hetero-dimeric complex, CAD/ICAD. Comparison with other structural homologues revealed that the PB1 domain of BEM1P, ubiquitin-like domain of BAG6 and ubiquitin are structurally similar proteins. Our homo-dimeric structure of the CIDE-N domain of FSP27 will provide important information that will enable better understanding of the function of FSP27.

1. Introduction

DNA fragmentation factor 40 and 45 (called DFF40/45), which are hetero-dimeric complexes, have been identified as the main executor and regulator of apoptotic DNA fragmentation, which is the best known biochemical hallmark of apoptotic cell death [1–4]. DFF40 (CAD in mouse) and DFF45 (ICAD in mouse) contain a common domain known as the CIDE domain, which is a protein interaction module of ~90 amino acid residues [5,6]. After discovering DFF40 and DFF45, CIDE-containing proteins including CIDE-A, CIDE-B and CIDE-3 (FSP27 in mouse) were identified based on their sequence homology [7,8]. Five CIDE-containing proteins have been identified in mammals to date, DFF40, DFF45, CIDE-A, CIDE-B, and CIDE-3 (called FSP27 in mouse). Splicing variants of CIDE-3 and DFF45 have also been identified and named CIDE-3α and DFF35, respectively [8,9]. Drep1, Drep2, Drep3, and Drep4 are CIDE-containing proteins in fly [7,10]. Although no clear evidence has been presented, the nuclease activity of Drep2 was recently reported and shown to be inhibited by Drep3 via tight interaction with CIDE domains [11].

Previous biochemical studies showed that all CIDE-containing proteins are involved in apoptosis. However, several current studies including a knock-out mouse study showed that CIDE-A, CIDE-B, and CIDE-3 localize to lipid droplets and the endoplasmic reticulum and are involved in lipid metabolism [12–15]. Because the disruption of lipid metabolism results in development of metabolic disorders such as diabetes, obesity and cardiovascular diseases, CIDE-containing proteins have been suggested as novel targets for therapeutic intervention of metabolic disorders.

FSP27 (CIDE-C in humans) is particularly involved in the regulation of lipid droplet (LD) size and lipid storage during lipid metabolism. This protein contains two CIDE domains at the N-terminus and C-terminus. Since CIDE-containing proteins (including FSP27) perform critical roles in apoptosis and lipid metabolism and are associated with many human diseases such as cancer, aging, diabetes, and obesity, studies of CIDE domains and CIDE-containing proteins are of great biological importance [16,17]. Although several CIDE domains and hetero-dimeric complex structures have been reported, no structural information is available for the homo-oligomeric complex of the CIDE domain [18–22]. Structural studies of many CIDEs are essential for understanding the molecular basis of lipid metabolism as well as apoptosis. Here, we report the crystal structure of the CIDE-N domain of FSP27 at a resolution of 2.0 Å. Although the CIDE-N domain of FSP27 has a typical α/β roll fold with two α helices and five (or four) β strands similar to other CIDEs, the high resolution structure reveals a possible biologically important homo-dimeric interface. The interface is similar to that formed by the hetero-dimeric complex between CAD and ICAD [21]. However, there are massive interactions formed by more highly charged residues. Comparison with other structural homologues revealed that the PB1 domain of BEM1P, ubiquitin-like domain of BAG6 and ubiquitin are structurally similar proteins.

* Corresponding author. Address: Department of Biochemistry, School of Biotechnology, Yeungnam University, South Korea. Fax: +82 053 810 4769.
E-mail address: hyunho@ynu.ac.kr (H.H. Park).

0006-291X/$ - see front matter © 2013 Elsevier Inc. All rights reserved.
http://dx.doi.org/10.1016/j.bbrc.2013.09.018

The first homo-dimeric structure of the CIDE-N domain of FSP27 will provide important information enabling understanding of the function of FSP27 in lipid metabolism, especially lipid droplet (LD) growth and apoptosis.

2. Materials and methods

2.1. Sequence alignment

The amino acid sequence of CIDEs was analyzed using Clustal W (http://www.ebi.ac.kr/Tools/clustalw2/index.html).

2.2. Protein expression and purification

The expression and purification methods used in this study have been described in detail elsewhere. Briefly, FSP27 (amino acid 32–120) was expressed in *Escherichia coli* BL21 (DE 3) under overnight induction at 20 °C. The protein contained a carboxyl terminal His-tag and was purified by nickel affinity and gel filtration chromatography using a 200 gel filtration column 10/30 (GE healthcare) that had been pre-equilibrated with a solution of 20 mM Tris–HCl at pH 8.0 and 500 mM NaCl. The protein was then concentrated to 7–8 mg/ml.

2.3. Crystallization and data collection

The crystallization conditions were initially screened at 20 °C by the hanging drop vapor-diffusion method using various screening kits. Initial crystals were grown on the plates by equilibrating a mixture containing 1 μl of protein solution (7–8 mg/ml protein in 20 mM Tris–HCl at pH 8.0, 500 mM NaCl) and 1 μl of a reservoir solution containing 28% polyethylene glycol (PEG) 1.500, 20 mM MMT buffer/NaOH pH 6.2 against 0.4 ml of reservoir solution. Crystallization was further optimized by searching over a range of concentrations of protein and precipitant and pH ranges. The diffraction data set was collected at the BL-4A beamline of Pohang Accelerator Laboratory (PAL), Republic of Korea. Data processing and scaling was carried out in the HKL2000 package (28). A 2.0 Å native data set was collected.

2.4. Structural determination and analysis

The molecular-replacement (MR) phasing method was used with the program *Phaser* [23] and a CIDE domain of human CIDE-B (PDB code 1d4b) [20], which has 31% amino-acid sequence homology with the CIDE-N domain of FSP27 as a search model. Probable MR solutions with rotation-function and translation function *Z*-scores of 6.1 and 10.2, respectively, for one monomer, and 6.8 and 21.8, respectively, for another monomer were initially obtained. Model building and refinement were performed using *COOT* [24] and *Refmac5* [25], respectively. Water molecules were added automatically with the ARP/wARP function in Refmac5 and then examined manually for reasonable hydrogen bonding possibilities. The quality of the model was checked using PROCHECK [26]. Ribbon diagrams and molecular surface representations were generated using the Pymol program [27].

2.5. Protein data bank accession codes

Coordinates and structure factors have been deposited in the RCSB Protein Data Bank. The PDB ID code is 4MAC.

3. Results and discussion

3.1. Structure of FSP27 CIDE-N domain

The CIDE domain is a protein interacting module of ~90 amino acids. Five CIDE-containing proteins have been identified in mammals including CIDE-A, CIDE-B, CIDE-3 (FSP27 in mouse), DFF40 (CAD in mouse), and DFF45 (ICAD in mouse). All CIDE domains contain central hydrophobic residues and several charged residues that are critical for formation of the hetero-dimeric complex (Fig. 1A). FSP27 contains two CIDE domains known as CIDE-N and CIDE-C. The CIDE-N domain is known to bind to several proteins, including Plin1, and to be directly involved in lipid droplet growth [28]. To better understand the function of FSP27 in lipid metabolism, we purified the CIDE-N domain of FSP27 using affinity chromatography followed by gel-filtration chromatography. The FSP27 CIDE-N domain eluted at approximately 14 ml, which corresponds to a molecular weight of around 24,000 Da, indicating that this domain exists in dimeric form in solution (Fig. 1B). After intensive crystallographic studies, the 2.0 Å high resolution crystal structure of the FSP27 CIDE-N domain was solved using a molecular replacement (MR) method and refined to an R_{work} of 22.4% and R_{free} of 29.2%. The high resolution structure of FSP27 CIDE-N showed that it comprises two helices, α1 and α2, and four strands, β1–β5, which form the typical α/β roll fold characteristic of the CIDE domains (Fig. 1C). There was one dimer (or two monomers) in the asymmetric unit, which was referred to as chain A and chain B (Fig. 1C). A model of chain A was built from residue 38 to residue 119, while that of chain B was built from residue 42 to residue 119. Overall, 97.44% of the residues were located in the most favorable region, while 2.56% were in the allowed regions of the Ramachandran plot. The data collection and refinement statistics are summarized in Table 1. Two chains formed an asymmetric dimer. Helix α2 was obviously detected and strand β4 was not well-defined in the structure of the FSP27 CIDE-N domain (Figs. 1C and 2A).

3.2. Comparison with other structural homologues

A typical CIDE domain fold is an α/β roll fold with two α helices and five β strands. Despite having the typical fold of CIDE domains, several CIDEs, including DFF40 CIDE and ICAD CIDE, do not contain a distinct α2 helix, which is the shortest helix. In addition, strand β4 was replaced by a flexible loop in DFF40 CIDE, DFF45 CIDE, ICAD CIDE, and CIDE-A. The structure of the FSP27 CIDE-N domain exhibited a typical CIDE domain fold that contains the α2 helix but not strand β4 (Fig. 2A). The two helices comprising residues 62–74 and 94–101 are indicated as α1 and α2. The four strands comprising the residues 43–48, 55–60, 81–85, and 106–110 are indicated as β1, β2, β3, and β5, respectively (Fig. 2A). Missing β4 was shown as (β4).

A structural homology search with *DALI* [29] revealed that the FSP27 CIDE-N domain is highly similar to the PB1 domain and ubiquitin-like domain, as well as other CIDE domains (Table 2). The top six matches, which had *Z*-scores of 8.6–6.3, were CIDE-A (PDBid: 2eel), PB1 domain of BEM1P (PDBid: 2kfk), CAD (PDBid: 1f2r-I), ICAD (PDBid: 1f2r-C), ubiquitin-like domain (UBL) of BAG6 (PDBid: 4eew), and ubiquitin (PDB id: 2g3q). Detection of the PB1 domain and ubiquitin domain as structurally similar to the CIDE-N domain of FSP27 indicates that the structure of CIDE is relatively close to that of the PB1 domain and ubiquitin domain.

Pair-wise structural alignments of the FSP27 CIDE-N domain and structural homologues showed that the length and orientation of α2 helices in FSP27 differed slightly from those of the others (Fig. 2A–F). For example, when compared with CAD, BAG6, and ubiquitin, the α2 helice of FSP27 showed differences in orientations (Fig. 2D–F). The

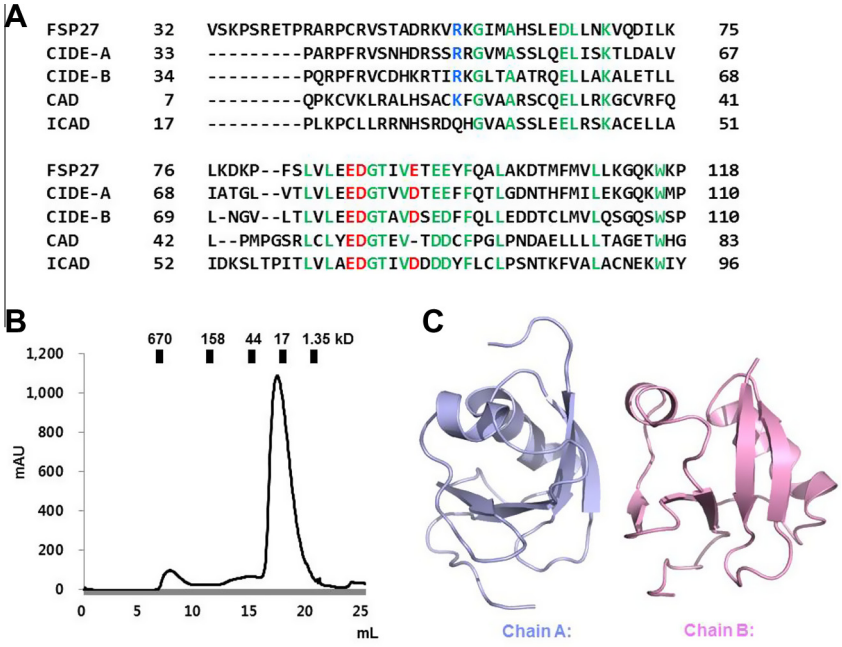

Fig. 1. Crystal structure of the FSP27 CIDE-N domain. (A) Sequence alignment of the FSP27 CIDE-N domain with other CIDE domains. Conserved residues are shown in green. Critical residues for the protein–protein interaction identified in previous studies are shown in blue for basic residues and red for acidic residues. (B) Multi-angle light scattering (MALS) measurement of the FSP27 CIDE-N domain showing the absolute molecular mass of the protein. The *x*-axis and *y*-axis indicate the elution volume and molecular mass respectively. (C) Ribbon diagram of the FSP27 CIDE-N domain. Chain A and Chain B are shown separately. (For interpretation of the references to color in this figure legend, the reader is referred to the web version of this article.)

Table 1
Crystallographic statistics.

Data collection	Native
Space group	$P3_2$
Cell dimensions	
a, *b*, *c*	63.3 Å, 63.3 Å, 37.6 Å
γ	120.0°
Resolution	50–2.0 Å
R_{sym}[a]	12.6% (78.8%)
Mean $I/\langle I \rangle$[a]	27.5 (2.9)
Completeness[a]	98.9% (99.4%)
Redundancy[a]	5.1 (5.0)
Refinement	
Resolution	30–2.0 Å
No. of reflections used (completeness)	10,752 (99%)
R_{work}/R_{free}	22.4%/29.2%
No. atoms	
Protein	1288
Water and other small molecules	74
Average B-factors	
Protein	31.5 Å^2
Water and other small molecules	36.0 Å^2
R.M.S. Deviations	
Bond lengths	0.022 Å
Bond angles	1.972°
Ramachandran plot	
Most favored regions	97.44%
Additional allowed regions	2.56%

[a] Highest resolution shell is shown in parentheses.

PB1 domain of BEM1P contains a relatively longer α2 helix (Fig. 2C). Due to the structural similarity between the CIDE domain and PB1 domain and UBL domain, functional characterization and comparison of those domains will be interesting.

3.3. Dimer interface within the FSP27 CIDE-N domain

The structure of the FSP27 CIDE-N domain reveals interesting insights into the homo-dimeric interfaces. The two FSP27 CIDE-N domains in the asymmetric unit are packed as an asymmetric dimer with an interface composed predominantly of electrostatic interaction (Fig. 3). A total dimer surface buries 968 Å^2 (a monomer surface area of 484 Å^2), which represents 9.1% of the dimer surface area. The principal contacts are made by R46, R55 and K56 (basic patch) from one FSP27 molecule (chain A) and by E87, D88 and E93 (acidic patch) from the second molecule (chain B) (Fig. 3). Among the acidic patch residues on chain A, R46 forms a salt bridge with E87 and D88 on chain B. K56 also forms a salt bridge with E93. Several H-bonds are also formed and contribute to stabilization of the dimer. G57 and R55 from chain A can form an H-bond with I91 and E87 from chain B, respectively. Because the isolated FSP27 CIDE-N behaves as a dimer in solution, the stoichiometry of FSp27 CIDE-N is that of a dimer, which might be critical for the biological activity of FSP27. The relationship between homo-dimerization and the function of FSP27 should be investigated in future studies.

3.4. Comparison of homo-dimeric interface with hetero-dimeric interface formed by the CIDE domain

Because the hetero-dimeric structure of CIDE domains between CAD (DFF40) and ICAD (DFF45) was previously solved [21], we compared the hetero-dimeric structure with the current homo-dimeric structure. The CAD/ICAD complex was well-superimposed with the current homo-dimeric structure with a root mean square deviation (R.M.S.D.) of 2.8 Å (Fig. 4A). The superimposition study also indicated that the orientation of the interface formed by the homo-dimeric complex was similar to that formed by the hetero-dimeric complex. Analysis of the interface formed by CAD/ICAD showed that the main force was a salt bridge formed by R39 on CAD and D71 on ICAD (Fig. 4B). There was also an H-bond between K21 and I69. Although K21 on CAD, which is aligned to R55 in FSP27, and D71 on ICAD, which is aligned to E93 in FSP27, contribute to the formation of the hetero-dimeric complex, the main residue in the hetero-dimeric complex is R39, which is aligned to uncharged residue I73 in FSP27, indicating that the homo-dimeric

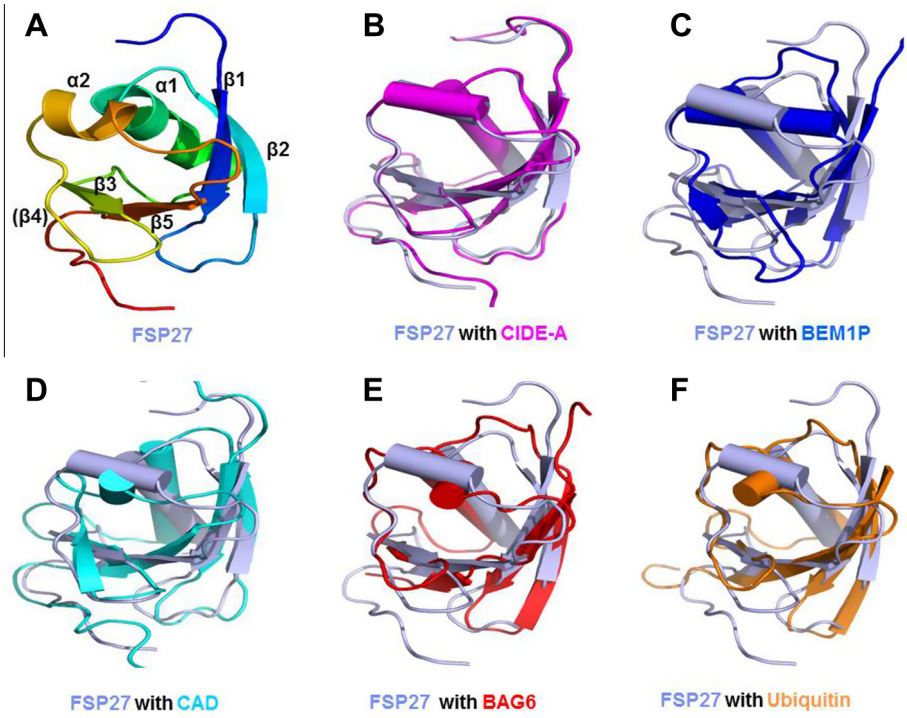

Fig. 2. Superposition of the FSP27 CIDE-N domain with their structural homologues. (A) Ribbon diagram of monomeric FSP27 CIDE-N domain. The chain from the N to the C-termini is colored from blue to red. Helices and sheets are labeled. The FSP27 CIDE-N domain and five structural homologues are superimposed pairwise. The FSP27 CIDE-N domain is light blue and its counterparts are magenta for CIDE-A (B), blue for the BEM1P BP1 domain (C), cyan for CAD (D), red for the BAG6 UBL domain (E), and orange for ubiquitin (F). (For interpretation of the references to color in this figure legend, the reader is referred to the web version of this article.)

Table 2
Structural similarity search using DALI.

Proteins and accession numbers	*Z*-score	RMSD (Å)	Identity (%)	References
CIDE-A (2eel)	8.6	1.21	54	Not published
BEM1P PB1 domain (2kfk)	6.3	1.98	15	[30]
CAD (1f2r-I)	8.5	1.99	34	[21]
ICAD (1f2r-C)	7.5	2.62	24	[21]
BAG6 UBL domain (4eew)	6.9	2.03	9	Not published
Ubiquitin (2g3q)	7.5	2.07	15	[31]

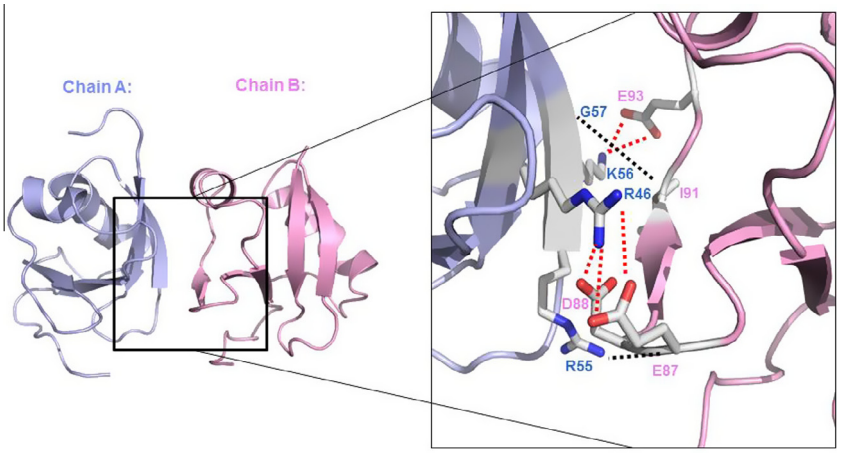

Fig. 3. Dimeric interface of the structure of the FSP27 CIDE-N domain. The dimeric structure is shown on the left side and a close-up view of the interacting residues in the interface between the two dimers is shown on the right side. The residues involved in the contact are shown in blue (from chain A) and pink (from chain B). Salt bridges formed between one chain and its counterpart are shown as red-dashed lines. H-bonds are shown as black-dashed lines. (For interpretation of the references to color in this figure legend, the reader is referred to the web version of this article.)

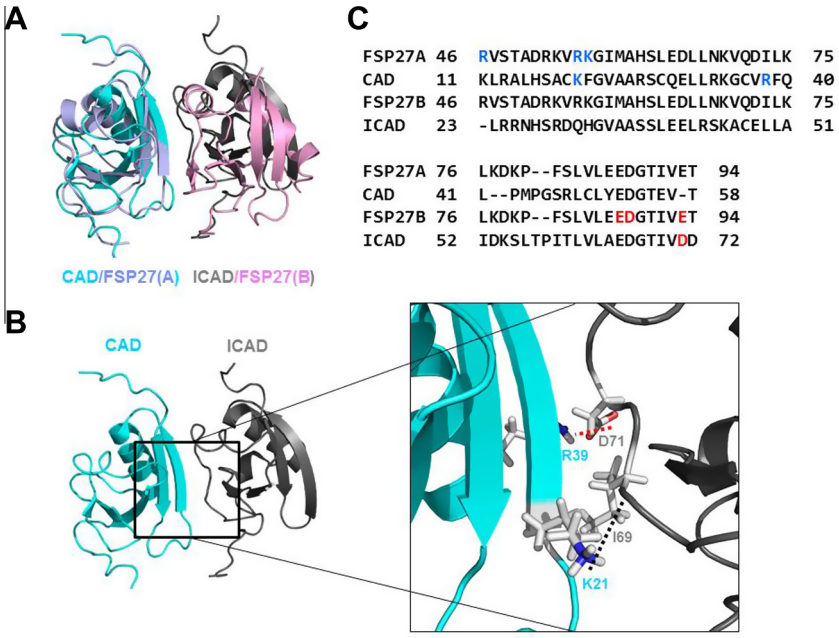

Fig. 4. Comparison with hetero-dimeric CIDE domain complex. (A) Superposition of homo-dimeric FSP27 with hetero-dimeric CAD CIDE/ICAD CIDE complex. (B) The hetero-dimeric structure of CAD CIDE/ICAD CIDE is shown on the left side. Close-up view of the interacting residues in the interface between the two dimers is shown on right side. The residues involved in the contact are shown. Salt bridges and H-bonds are shown as red-dashed and black-dashed lines, respectively. (C) Critical residues for the hetero-dimeric interaction for CAD CIDE/ICAD CIDE and homo-dimeric interaction for the FSP27 CIDE-N domain are shown. Blue and red indicate basic and acidic residues, respectively. (For interpretation of the references to color in this figure legend, the reader is referred to the web version of this article.)

complex uses more charged residues to form massive salt-bridges in the interface (Fig. 4B and C).

The structure of the FSP27 CIDE-N domain provides the first step towards elucidating the function of FSP27 in the lipid droplet growth and dimerization mechanism of FSP27, which is similar to the hetero-dimerization formed by CAD/ICAD. The dimerization and larger interactions detected at the homo-dimer of the FSP27 CIDE-N domain might be important for the function of FSP27 in lipid metabolism.

Acknowledgments

This study was supported by a National Research Foundation of Korea (NRF) grant funded by the Korean government (MEST) (2013009083).

References

[1] A. Batistatou, L.A. Greene, Internucleosomal DNA cleavage and neuronal cell survival/death, J. Cell Biol. 122 (1993) 523–532.
[2] H. Sakahira, M. Enari, S. Nagata, Functional differences of two forms of the inhibitor of caspase-activated DNase, ICAD-L, and ICAD-S, J. Biol. Chem. 274 (1999) 15740–15744.
[3] S.L. Sabol, R. Li, T.Y. Lee, R. Abdul-Khalek, Inhibition of apoptosis-associated DNA fragmentation activity in nonapoptotic cells: the role of DNA fragmentation factor-45 (DFF45/ICAD), Biochem. Biophys. Res. Commun. 253 (1998) 151–158.
[4] H.H. Park, Fifty C-terminal amino acid residues are necessary for the chaperone activity of DFF45 but not for the inhibition of DFF40, BMB Rep. 42 (2009) 713–718.
[5] N. Inohara, T. Koseki, S. Chen, X. Wu, G. Nunez, CIDE, a novel family of cell death activators with homology to the 45 kDa subunit of the DNA fragmentation factor, EMBO J. 17 (1998) 2526–2533.
[6] X. Liu, H. Zou, C. Slaughter, X. Wang, DFF, a heterodimeric protein that functions downstream of caspase-3 to trigger DNA fragmentation during apoptosis, Cell 89 (1997) 175–184.
[7] N. Inohara, G. Nunez, Genes with homology to DFF/CIDEs found in *Drosophila melanogaster*, Cell Death Differ. 6 (1999) 823–824.
[8] L. Liang, M. Zhao, Z. Xu, K.K. Yokoyama, T. Li, Molecular cloning and characterization of CIDE-3, a novel member of the cell-death-inducing DNA-fragmentation-factor (DFF45)-like effector family, Biochem. J. 370 (2003) 195–203.
[9] J. Gu, R.P. Dong, C. Zhang, D.F. McLaughlin, M.X. Wu, S.F. Schlossman, Functional interaction of DFF35 and DFF45 with caspase-activated DNA fragmentation nuclease DFF40, J. Biol. Chem. 274 (1999) 20759–20762.
[10] O.K. Park, H.H. Park, A putative role of Drep1 in apoptotic DNA fragmentation system in fly is mediated by direct interaction with Drep2 and Drep4, Apoptosis 18 (2013) 385–392.
[11] O.K. Park, H.H. Park, Dual apoptotic DNA fragmentation system in the fly: Drep2 is a novel nuclease of which activity is inhibited by Drep3, FEBS Lett. 586 (2012) 3085–3089.
[12] N. Nishino, Y. Tamori, S. Tateya, T. Kawaguchi, T. Shibakusa, W. Mizunoya, K. Inoue, R. Kitazawa, S. Kitazawa, Y. Matsuki, R. Hiramatsu, S. Masubuchi, A. Omachi, K. Kimura, M. Saito, T. Amo, S. Ohta, T. Yamaguchi, T. Osumi, J. Cheng, T. Fujimoto, H. Nakao, K. Nakao, A. Aiba, H. Okamura, T. Fushiki, M. Kasuga, FSP27 contributes to efficient energy storage in murine white adipocytes by promoting the formation of unilocular lipid droplets, J. Clin. Invest. 118 (2008) 2808–2821.
[13] S.C. Lin, P. Li, CIDE-A, a novel link between brown adipose tissue and obesity, Trends Mol. Med. 10 (2004) 434–439.
[14] Z. Zhou, S. Yon Toh, Z. Chen, K. Guo, C.P. Ng, S. Ponniah, S.C. Lin, W. Hong, P. Li, Cidea-deficient mice have lean phenotype and are resistant to obesity, Nat. Genet. 35 (2003) 49–56.
[15] J.Z. Li, J. Ye, B. Xue, J. Qi, J. Zhang, Z. Zhou, Q. Li, Z. Wen, P. Li, Cideb regulates diet-induced obesity, liver steatosis, and insulin sensitivity by controlling lipogenesis and fatty acid oxidation, Diabetes 56 (2007) 2523–2532.
[16] T.G. Cotter, Apoptosis and cancer: the genesis of a research field, Nat. Rev. Cancer 9 (2009) 501–507.
[17] T. Yonezawa, R. Kurata, M. Kimura, H. Inoko, Which CIDE are you on? Apoptosis and energy metabolism, Mol. Biosyst. 7 (2011) 91–100.
[18] S.M. Lee, H.H. Park, General interaction mode of CIDE:CIDE complex revealed by a mutation study of the Drep2 CIDE domain, FEBS Lett. 587 (2013) 854–859.
[19] K. Fukushima, J. Kikuchi, S. Koshiba, T. Kigawa, Y. Kuroda, S. Yokoyama, Solution structure of the DFF-C domain of DFF45/ICAD. A structural basis for the regulation of apoptotic DNA fragmentation, J. Mol. Biol. 321 (2002) 317–327.
[20] A.A. Lugovskoy, P. Zhou, J.J. Chou, J.S. McCarty, P. Li, G. Wagner, Solution structure of the CIDE-N domain of CIDE-B and a model for CIDE-N/CIDE-N interactions in the DNA fragmentation pathway of apoptosis, Cell 99 (1999) 747–755.
[21] T. Otomo, H. Sakahira, K. Uegaki, S. Nagata, T. Yamazaki, Structure of the heterodimeric complex between CAD domains of CAD and ICAD, Nat. Struct. Biol. 7 (2000) 658–662.
[22] P. Zhou, A.A. Lugovskoy, J.S. McCarty, P. Li, G. Wagner, Solution structure of DFF40 and DFF45 N-terminal domain complex and mutual chaperone activity of DFF40 and DFF45, Proc. Natl. Acad. Sci. USA 98 (2001) 6051–6055.
[23] A.J. McCoy, Solving structures of protein complexes by molecular replacement with *Phaser*, Acta Crystallogr. D Biol. Crystallogr. 63 (2007) 32–41.

[24] P. Emsley, K. Cowtan, Coot: model-building tools for molecular graphics, Acta Crystallogr. D Biol. Crystallogr. 60 (2004) 2126–2132.
[25] G.N. Murshudov, P. Skubak, A.A. Lebedev, N.S. Pannu, R.A. Steiner, R.A. Nicholls, M.D. Winn, F. Long, A.A. Vagin, REFMAC5 for the refinement of macromolecular crystal structures, Acta Crystallogr. D Biol. Crystallogr. 67 (2011) 355–367.
[26] R.A. Laskowski, J.A. Rullmannn, M.W. MacArthur, R. Kaptein, J.M. Thornton, AQUA and PROCHECK-NMR: programs for checking the quality of protein structures solved by NMR, J. Biomol. NMR 8 (1996) 477–486.
[27] W.L. Delano, The PyMol Molecular Graphics System, DeLano Scientific LLC, CA, USA, 2002.
[28] T.H. Grahn, Y. Zhang, M.J. Lee, A.G. Sommer, G. Mostoslavsky, S.K. Fried, A.S. Greenberg, V. Puri, FSP27 and PLIN1 interaction promotes the formation of large lipid droplets in human adipocytes, Biochem. Biophys. Res. Commun. 432 (2013) 296–301.
[29] L. Holm, C. Sander, Dali: a network tool for protein structure comparison, Trends Biochem. Sci. 20 (1995) 478–480.
[30] K. Ogura, T. Tandai, S. Yoshinaga, Y. Kobashigawa, H. Kumeta, T. Ito, H. Sumimoto, F. Inagaki, NMR structure of the heterodimer of Bem1 and Cdc24 PB1 domains from *Saccharomyces cerevisiae*, J. Biochem. 146 (2009) 317–325.
[31] K.A. Swanson, L. Hicke, I. Radhakrishnan, Structural basis for monoubiquitin recognition by the Ede1 UBA domain, J. Mol. Biol. 358 (2006) 713–724.